Human Molecular Genetics, 2009, Vol. 18, No. 12 **2127–2139**
doi:10.1093/hmg/ddp136
Advance Access published on March 20, 2009

Astrocytic protection of spinal motor neurons but not cortical neurons against loss of Als2/alsin function

A. Jacquier[1], S. Bellouze[1], S. Blanchard[2], D. Bohl[2] and G. Haase[1,*]

[1]Laboratory of Motor Neuron Disease Modeling and Therapy, Institut de Biologie du Développement de Marseille Luminy, Université Aix-Marseille, Case 907, Parc scientifique de Luminy, F-13273 Marseille cedex 09, France and [2]Institut Pasteur, INSERM U622, Paris, France

Received December 3, 2008; Revised March 1, 2009; Accepted March 18, 2009

Three neurodegenerative diseases affecting upper and/or lower motor neurons have been associated with loss of *ALS2/Alsin* function: juvenile amyotrophic lateral sclerosis, primary lateral sclerosis and infantile-onset ascending hereditary spastic paralysis. The distinct neuronal vulnerability and the role of glia in these diseases remains, however, unclear. We here demonstrate that alsin-depleted spinal motor neurons can be rescued from defective survival and axon growth by co-cultured astrocytes. The astrocytic rescue is mediated by a soluble protective factor rather than by cellular contact. Cortical neurons are intrinsically as vulnerable to alsin depletion as spinal motor neurons but cannot be rescued by co-cultured astrocytes. To our knowledge, these data provide the first example of non-cell-autonomous glial effects in a recessive form of motor neuron disease and a potential rationale for the higher vulnerability of upper versus lower motor neurons in *ALS2/Alsin*-linked disorders.

INTRODUCTION

Motor neuron diseases represent a spectrum of neurodegenerative disorders with considerable clinical and genetic heterogeneity (reviewed in 1,2). Recessive mutations in *ALS2/Alsin* have been reported in juvenile forms of amyotrophic lateral sclerosis (ALS2, OMIM 205100), primary lateral sclerosis (JPLS, OMIM 606353) and infantile-onset ascending hereditary spastic paralysis (IAHSP, OMIM 607225) (reviewed in 3,4). ALS affects both upper motor neurons in cerebral cortex and lower motor neurons in spinal cord and brainstem, whereas primary lateral sclerosis (PLS) classically affects only upper motor neurons. IAHSP resembles PLS but with an earlier onset, a slowly progressive ascending evolution and a severe degeneration of the pyramidal tracts (5). Alsin is a 1657 amino acid/184 kDa protein harbouring RCC1-like motifs modulating membrane association (6,7), a DH/PH domain acting as a guanine nucleotide exchange factor (GEF) for the GTPase Rac1 (8–12) and a VPS9 GEF domain for Rab5 (8,10), see Figure 1A. To date, fourteen *ALS2* mutations have been identified: the vast majority in IAHSP (13–17), three in JPLS (18,19) and two in ALS2 with predominant upper motor neuron symptoms (18,20). These mutations represent small deletions, non-sense or missense mutations and are scattered along the *ALS2* open reading frame.

In the absence of a genotype/phenotype correlation and of human autopsy studies, the greater vulnerability of upper versus lower motor neurons in ALS2, JPLS and IAHSP remains unexplained. Studies in alsin knockout mice (21–26) have not resolved this issue. One mouse line displayed no histological signs of neurodegeneration (21), whereas another mainly exhibited signs of lower motor neuron degeneration such as progressive loss of ventral root axons, skeletal muscle denervation and motor unit remodelling (22). Conversely, only upper motor neurons were affected in three lines, as attested by atrophy of cell bodies in cortical layer 5 (23) and degeneration of corticospinal axons in the dorsal (24) or dorsolateral (25) columns of the spinal cord. In a sixth line of alsin knockout mice, both upper and lower motor neurons showed signs of degeneration (26). These discrepancies might be due to differences in histopathological procedures and mouse genetic backgrounds or to the persistence of functional alsin transcripts in some knockout lines

*To whom correspondence should be addressed. Tel:+33 491269278/+33 673238113; Fax:+33 491269757; Email: haase@ibdml.univ-mrs.fr

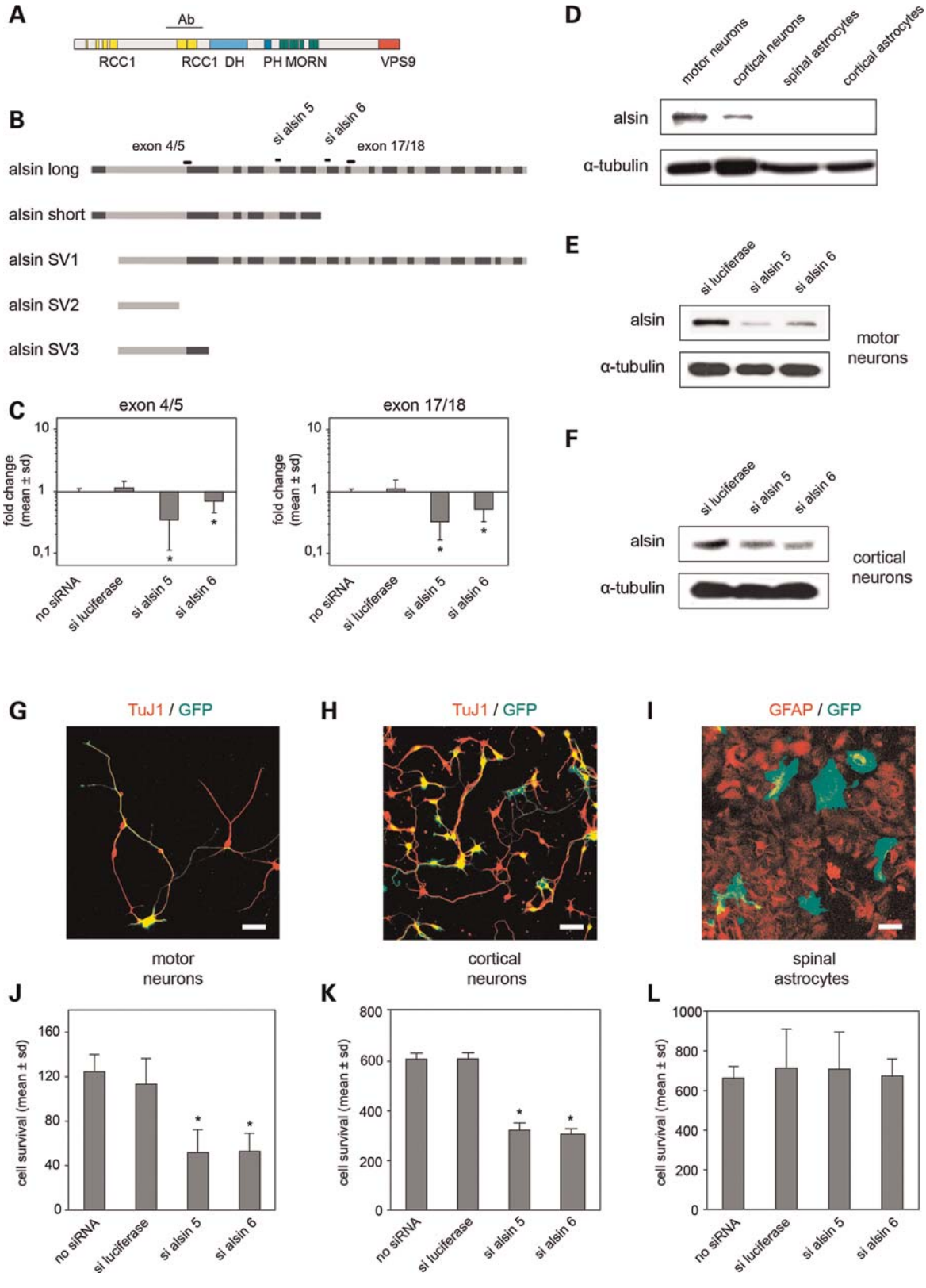

Figure 1. RNAi-mediated alsin knockdown in neuronal and astrocytic cultures. (**A**) Schematic representation of alsin full-length protein and its predicted domains. RCC1: regulator of chromosome condensation. DH: dbl homology. PH: pleckstrin homology. MORN: membrane occupation and recognition nexus. VPS9: vesicular protein sorting 9. The epitope of amino acid 452–668 recognized by the anti-alsin antibody (Ab) is also represented. (**B**) Schematic

(26). The first objective of this study was therefore to compare the vulnerability of different types of neurons to loss-of-alsin function.

Glial cells play an important role in the pathological degeneration of motor neurons (reviewed in 1,2). Histopathological studies in sporadic ALS and mutant SOD1-linked familial ALS have shown that gliosis, i.e. proliferation and activation of astrocytes and microglia, accompanies the degeneration of motor neuron cell bodies and their axons (27–29). Genetic studies have further demonstrated that glial cells can exacerbate the neurodegenerative process. In transgenic mice, mutant SOD1 expression in microglia and astrocytes determined disease progression (2,30). *In vitro*, mutant SOD1 expressing astrocytes increased the cell death of co-cultured motor neurons isolated from spinal cord or differentiated from embryonic stem cells (31–33), and mutant spinal motor neurons showed increased vulnerability to cell death triggers produced by glia (reviewed in 34,35). *In vivo*, astrogliosis and microglial activation were reported in one line of alsin knockout mice (22) but were absent in another (26). The second objective of this study was thus to investigate the potential contribution of glia to alsin-linked neurodegeneration.

In the developing nervous system, alsin expression starts at embryonic age (mouse E9.5) and increases until early postnatal age (36). In neurons, alsin localizes to early endosomes in the neuronal soma (8,10) and to punctuate structures in neurites (10,37) and growth cones (11,38). Alsin has been implicated in endocytosis (8,10,23), micropinocytosis (39) and membrane trafficking (10). Its role in neuronal growth or maintenance is, however, not fully understood. Various types of neurons from alsin knockout mice showed normal survival in baseline conditions (21,23,37,39) but increased cell death in response to oxidative stress (21) or excitotoxicity (37). More drastic effects were observed by alsin gene knockdown. Through RNAi-mediated alsin knockdown, we observed severe axon growth and survival defects in rat motor neurons (38). Injection of morpholino-antisense oligonucleotides against alsin into zebrafish resulted in perturbed spinal motor nerve outgrowth and swimming defects (26).

To investigate the role of alsin in neurons and glia, we here determined the alsin protein expression and the consequences of RNAi-mediated alsin depletion under defined *ex vivo* conditions. Our data show that mouse spinal motor neurons and cortical neurons both express alsin and are equally sensitive to cell death triggered by alsin depletion. In neuron–astrocyte co-cultures, cell bodies and axons of alsin-depleted spinal motor neurons are rescued by co-cultured astrocytes which do not express alsin. This rescue is mediated by a soluble protective factor rather than by cellular contact. No astrocytic rescue is observed for alsin-depleted cortical neurons. These data provide new hypotheses for the difference in vulnerability of upper and lower motor neurons in *ALS2*-linked and related neurodegenerative disorders.

RESULTS

Spinal motor neurons and cortical neurons show similar vulnerability to alsin depletion

To induce alsin loss-of-function in neurons, we used RNAi-mediated knockdown of alsin transcripts. The mouse CNS contains multiple alsin transcripts (Fig. 1B) generated by alternative splicing (18) and possibly also by alternative transcription initiation (26). Two long transcripts have been shown to be functional: the full length transcript (exons 1–34) which gives rise to the mature alsin 184 kDa protein and the SV1 transcript (exons 4–34) which can partially rescue mutant alsin zebrafish (26). Other reported alsin transcripts are of less certain relevance: the alsin short transcript (exons 1–13) does not yield a detectable protein and the very short transcripts SV2 and SV3 (26) lack the exons encoding the central and C-terminal GEF domains. To knockdown functional alsin transcripts in mice by RNA interference, we used chemically synthesized small interfering RNA (siRNA) targeting either exon 10 (si alsin 5) or exon 14 (si alsin 6). To study their catalytic efficiency, we transfected motor neurons of the NSC34 cell line (40) and analyzed them by quantitative reverse transcriptase–polymerase chain reaction (qRT–PCR) analysis. Levels of alsin transcripts containing exons 4/5 (full length, short, SV1, SV3) were found to be reduced to 0.34-fold of mock by si alsin 5 and to 0.69-fold by si alsin 6 (Fig. 1C, $P < 0.01$ as assessed by Student's *t*-test). Levels of alsin transcripts containing exons 17/18 (full length and SV1) were reduced to a similar extent by each siRNA (Fig. 1C). These data indicate that all known functional alsin transcripts are efficiently targeted by si alsin 5 and si alsin 6 siRNA.

We then studied the expression of alsin in embryonic spinal motor neurons and cortical neurons. After culture for 2 days *in vitro* (2 DIV), both types of neurons expressed full length 184 kDa protein (Fig. 1D) but not smaller alsin protein

representation of reported alsin transcripts and position of chemically synthesized siRNA duplexes used for alsin knockdown. Boxes indicate alsin exons 1–34. Primer pairs in exons 4/5 and 17/18 were used for quantitative reverse transcriptase–polymerase chain reaction (qRT–PCR) analysis of alsin expression. (**C**) qRT–PCR analysis showing efficient knockdown of alsin transcripts in NSC34 motor neurons. Levels of alsin transcripts containing exons 4/5 or 17/18 are normalized to those of acidic ribosomal phosphoprotein (ARPO). Values represent the fold change after transfection of NSC34 cells with no siRNA (set to 1), si luciferase, si alsin 5 or si alsin 6. $^*P < 0.01$ as assessed by Student's *t*-test. (**D**) Western blot analysis showing alsin protein expression in cultured spinal motor neurons and cortical neurons cultured for 2 DIV. Note absence of alsin expression in astrocytes cultured from spinal cord and cerebral cortex. Alsin (184 kDa) was detected with rabbit polyclonal antibodies in 40 μg protein extract per lane. After stripping, membranes were re-probed with an antibody against α-tubulin. (**E** and **F**) Western blot analyses showing alsin depletion in spinal motor neurons and cortical neurons electroporated with siRNAs si alsin 5 or si alsin 6. (**G**–**I**) Images of cultured spinal motor neurons (G), cortical neurons (H) and spinal astrocytes (I) at 2 DIV after co-electroporation of GFP vector and control siRNA. Counterstaining for neuronal β_{III}-tubulin (TuJ1, in red) or glial fibrillary acidic protein (GFAP, in red) illustrates high-transduction rate and purity of cultures. Scale bars: 50 μm. (**J**–**L**) Survival of transduced cells at 2 DIV determined in 96-well plates using an automated fluorescent plate reader. Alsin depletion in spinal motor neurons (J) causes a similar reduction in cell number as in cortical neurons (K). There is no such effect in spinal astrocytes (L). Diagrams show one representative experiment out of three. $^*P < 0.001$, *t*-test, $n = 8$ parallel wells per condition.

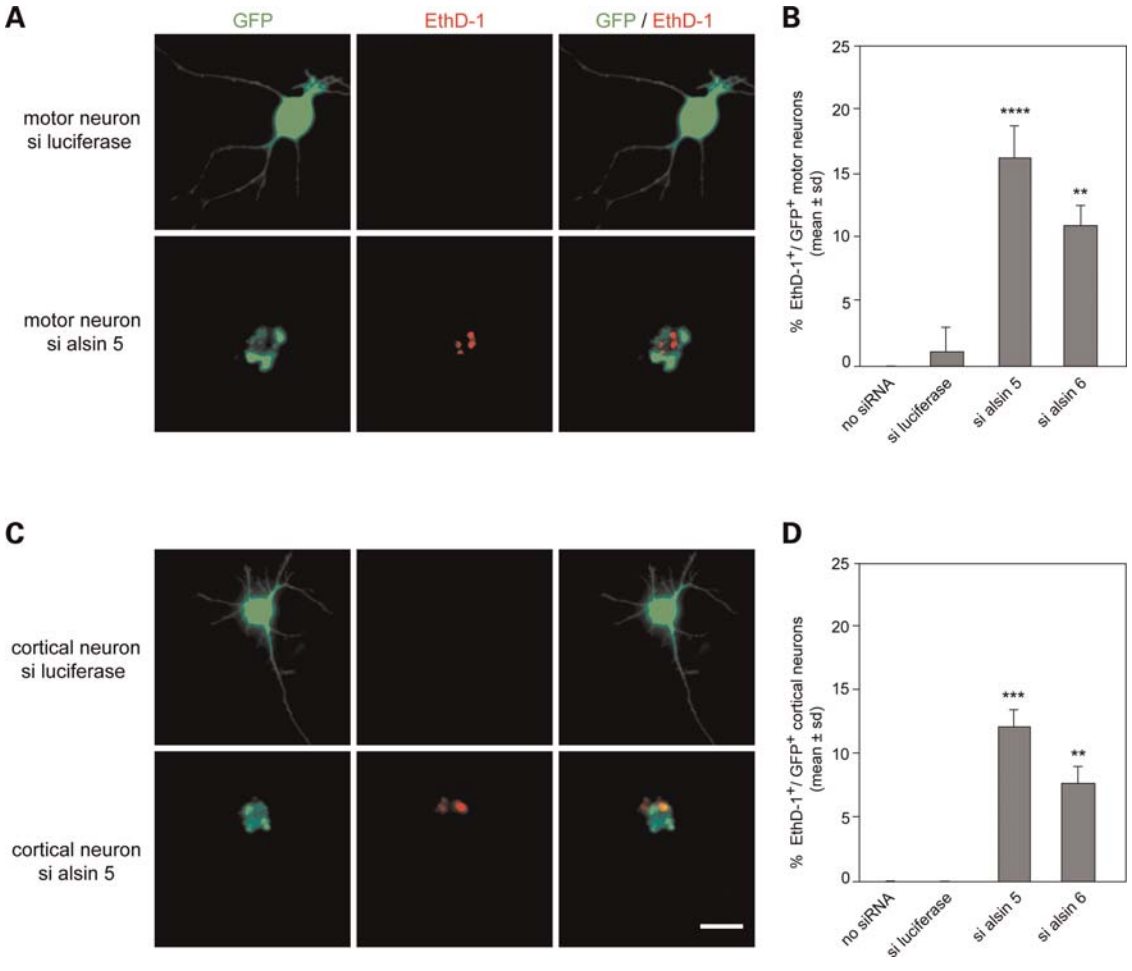

Figure 2. Cell death susceptibility of alsin-depleted spinal motor and cortical neurons. (**A**) Images of spinal motor neurons transduced with si alsin 5/GFP or si luciferase/GFP and labelled at 2 DIV with the cell death marker ethidium homodimer (EthD-1). (**B**) Diagram showing a significantly increased percentage of dying EthD-1/GFP-positive spinal motor neurons following alsin depletion. (**C**) Images of siRNA/GFP-transduced cortical neurons with a EthD-1 labelling. (**D**) Diagram showing significantly increased percentage of EthD-1/GFP double-positive cortical neurons following alsin depletion. Scale bars (A and C) represent 20 μm. Values (B and D) are mean ± SD from two independent experiments each performed in duplicate and represent ∼200 cells per condition. Student's *t*-test demonstrated statistical differences among values for spinal motor neurons (****$P < 0.0005$ si alsin 5 versus si luciferase, **$P < 0.02$ si alsin 6 versus si luciferase) and cortical neurons (***$P < 0.005$ si alsin 5 versus si luciferase, **$P < 0.02$ si alsin 6 versus si luciferase). Two-way ANOVA showed no statistical differences in cell death sensitivity of spinal motor neurons versus cortical neurons ($P > 0.5$) and efficiency of si alsin 5 versus si alsin 6 ($P > 0.5$).

isoforms corresponding to the short transcripts (data not shown), which is consistent with previous data (8,36). To knockdown alsin in motor and cortical neurons, we introduced the siRNAs (4 pmol/μl) by electroporation (37). Western blot analyses at 2 DIV demonstrated efficient depletion of alsin in both types of neurons (Fig. 1E and F). To analyze the effects of alsin depletion on neuronal survival, we co-electroporated a pCAGGS GFP expression plasmid together with the siRNAs (Fig. 1E and F). For unbiased survival analyses, the fluorescent neurons were cultured in 96-well plates, imaged with a plate reader, and their number determined with automated software (see Materials and Methods). At 2 DIV, the number of alsin-depleted spinal motor neurons was decreased to 46 ± 19% (si alsin 5, mean ± SD) and 47 ± 14% (si alsin 6, mean ± SD) in comparison with that of si luciferase-electroporated spinal motor neurons (Fig. 1G and J). In cortical neurons, alsin depletion (Fig. 1H and K) caused a similar reduction in survival (si alsin 5: 53 ± 5%, si alsin 6: 50 ± 3.6%, mean ± SD).

To further compare the vulnerability of both types of neurons, we determined their survival response to lower siRNA concentrations in the range of 0.13–4 pmol/μl. Motor and cortical neurons displayed a similar dose-dependant decrease in cellular survival to increasing concentrations of si alsin 5 (Supplementary Material, Fig. S1). To analyze whether the decrease in cellular survival reflected an increase in cell death, we assessed the proportion of dying neurons using ethidium homodimer-1 (EthD-1), a red-fluorescent DNA dye that selectively penetrates compromised membranes (Fig. 2A and C). In alsin-depleted spinal motor neuron cultures, the percentage of EthD-1/GFP-double positive cells at 2 DIV was 10–15-fold higher (si alsin 5: 16 ± 3%, si alsin 6: 11 ± 2%, mean ± SD) than in control cultures (mock: 0%, si luciferase: 1 ± 1%, $P < 0.025$, Student's *t*-test, Fig. 2B). Alsin depletion in cortical neurons induced a similar increase in the rate of cell death (Fig. 2D). Taken together, data on cellular survival and death thus indicate a similar vulnerability of spinal motor neurons and cortical neurons to loss-of-alsin function.

Astrocytic protection of alsin-depleted spinal motor neurons

To test the effects of astrocytes on the survival of alsin-depleted neurons, we prepared neuron/glia co-cultures. Spinal astrocytes were isolated from early post-natal spinal cord, cultured through two to three passages to 95% purity and established as monolayers. Western blot analysis showed that spinal astrocytes did not express alsin (Fig. 1D), in contrast to neurons. In accordance, their proliferation, survival and morphology were not modified by electroporation with si alsin 5 or si alsin 6 (Fig. 1I and L). These data are consistent with the reported lack of alsin expression in adult glia (8,36) and circumvented the need to use alsin-depleted or deficient astrocytes. Spinal motor neurons were then electroporated with si luciferase or si alsin 5 in combination with the GFP plasmid. Half of each neuronal suspension was then seeded on the astrocyte monolayer and the other half in empty wells (Fig. 3A and B). In co-cultures, the transduced spinal motor neurons differentiated and grew out long axons, whereas the astrocytes retained their typical morphology and GFAP expression (Fig. 3A). Spinal astrocytes had no significant effect on the survival of control motor neurons (Fig. 3C). In striking contrast, however, they completely rescued the survival of alsin-depleted spinal motor neurons (Fig. 3C, $P < 0.001$, *t*-test) and abrogated their pathological cell death, as judged from lacking EthD-1 labelling (data not shown). The rescue effect did not vary with the ratio of astrocytes to neurons. We conclude that astrocytes efficiently protect spinal motor neurons from alsin-induced cell death.

Astrocytic protection of alsin-depleted spinal motor neurons is mediated by a soluble factor

Astrocytes can enhance neuronal survival by providing structural, metabolic and trophic support and by regulating the extracellular concentration of neurotransmitters and ions (reviewed in 41,42). We therefore tested whether the observed astrocytic protection was mediated by membrane contact or by a soluble factor. To evaluate the influence of membrane contact, spinal astrocyte monolayers were fixed with ethanol (Fig. 4A) using a protocol that preserves cell surface molecules required for neuronal survival and neurite outgrowth (43). Ethanol-fixed astrocytes protected <13% of spinal motor neurons from alsin depletion-induced cell death (Fig. 4B, not significant), in contrast to the complete rescue exerted by viable astrocytes (Fig. 3C).

We next tested whether astrocytic protection is mediated by a soluble factor. For this purpose, we developed a co-culture system allowing factors to be continuously produced and to freely diffuse between cells (Fig. 4C). Spinal motor neurons were cultured on top of coverslips separated by wax stilts from spinal astrocyte monolayers on the bottom (44,45). Under these conditions, alsin-depleted spinal motor neurons were rescued, as estimated from normal survival of GFP fluorescent neurons (Fig. 4D) and absence of EthD-1/GFP-positive dead neurons (data not shown). This indicated that astrocytic rescue from alsin knockdown induced death is mediated by a diffusible factor. We reasoned that this rescue might be due to a protective factor released by astrocytes or a toxic

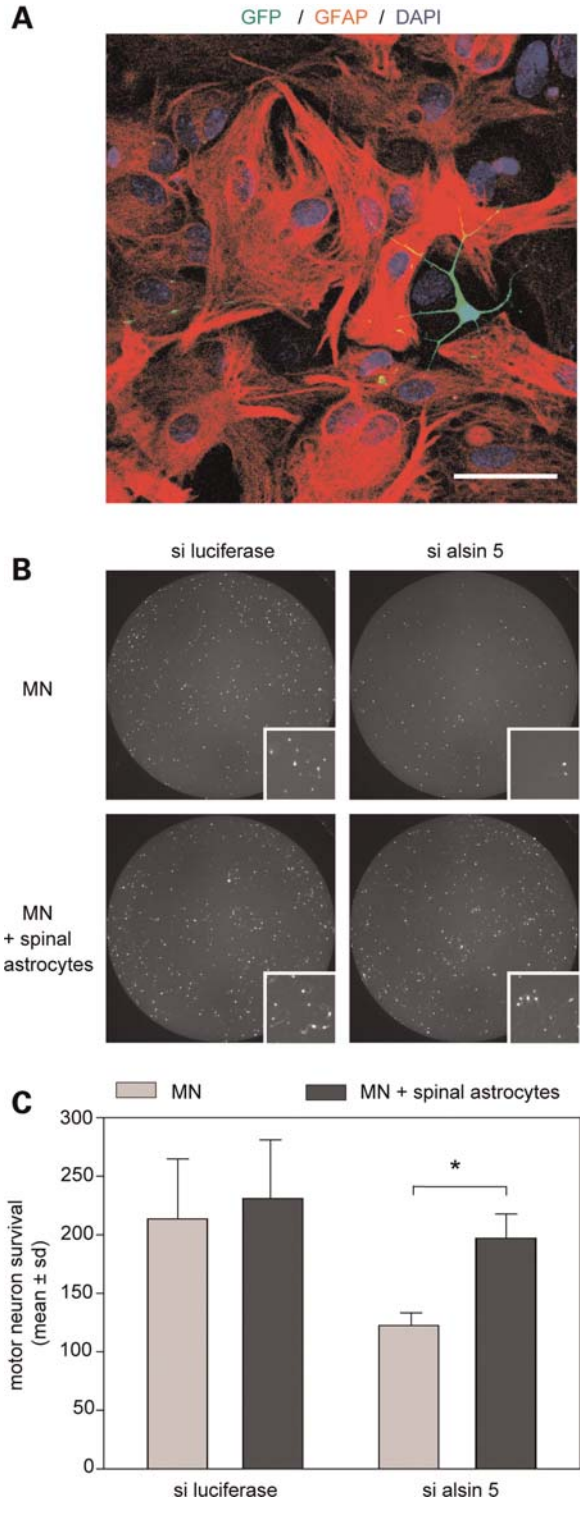

Figure 3. Astrocytes protect alsin-depleted spinal motor neurons against cell death. (**A**) Co-culture of electroporated spinal motor neurons (GFP, green) on a pre-established monolayer of spinal astrocytes (GFAP, red). Nuclei are stained with DAPI (blue). Scale bar: 50 μm. (**B**) Survival of control and alsin-depleted spinal motor neurons (GFP, white) cultured for 2 DIV in the presence or absence of co-cultured spinal astrocytes (not visible). Insets with zooms on the central area of the wells demonstrate reduction in neuronal survival after alsin depletion. (**C**) Protection of alsin-depleted spinal motor neurons (MN) by spinal astrocytes. Histograms show mean ± SD of individual experiments. $^{*}P < 0.02$ by Student's *t*-test. Each experiment was repeated twice.

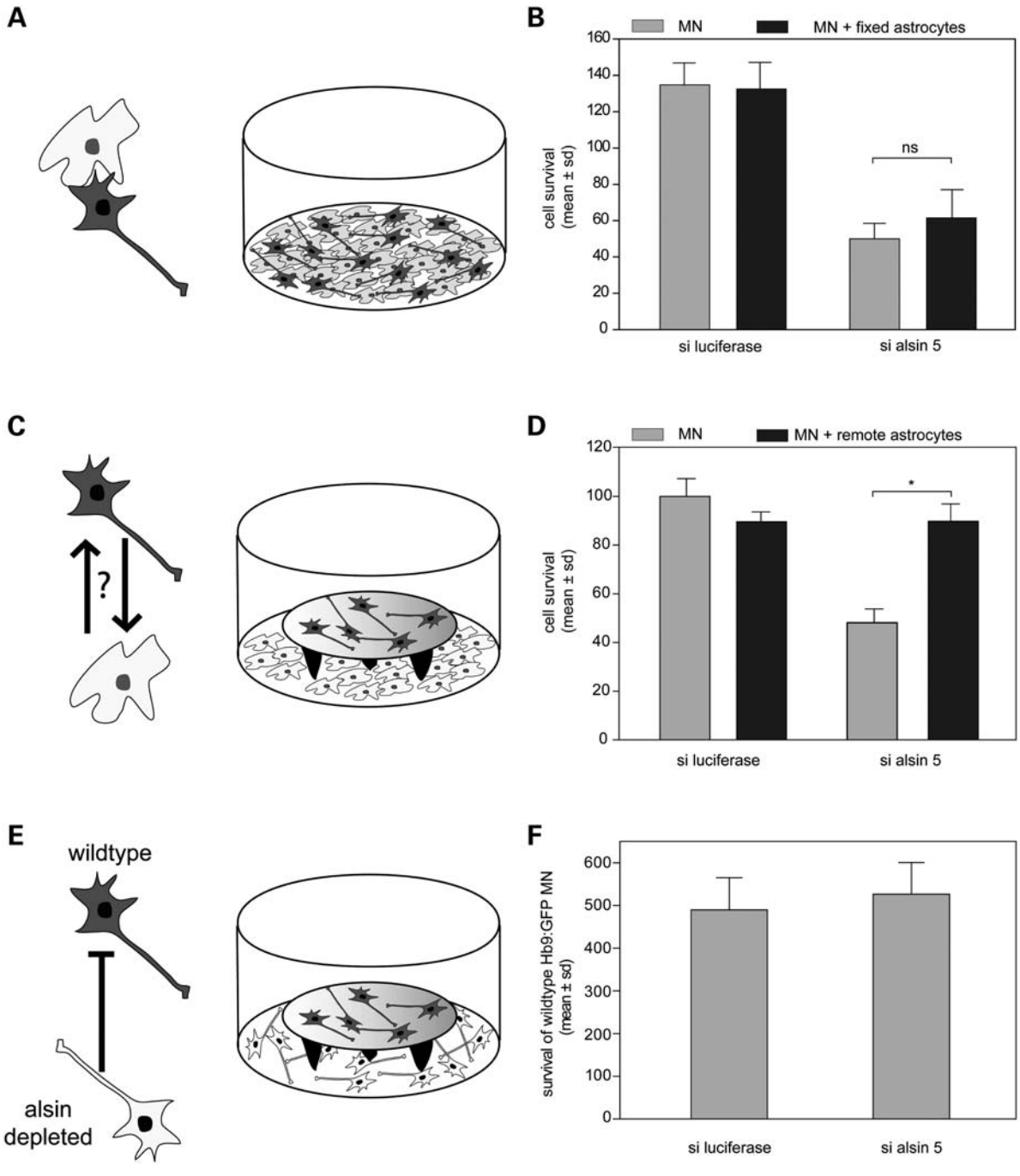

Figure 4. A soluble astrocyte-derived factor mediates protection of alsin-depleted spinal motor neurons. Hypothetic mechanisms, design of co-cultures and experimental data concerning protection of alsin-depleted spinal motor neurons (MN) by a membrane-bound astrocytic factor (**A** and **B**), a soluble factor released by astrocytes (**C** and **D**) or a toxic factor scavenged by astrocytes (**E** and **F**). (A) A membrane-bound astrocytic factor was searched in co-cultures of spinal motor neurons and spinal astrocytes fixed (or not) with ethanol. (B) Diagram showing that alsin-depleted spinal motor neurons are not significantly (ns) protected by ethanol-fixed astrocytes. (C) Release of a protective soluble factor by astrocytes tested in co-cultures of spinal motor neurons placed on coverslips on top of remote astrocyte monolayers. (D) Diagram showing that alsin-depleted spinal motor neurons are almost completely protected by remote astrocytes. $^{*}P < 0.005$ by Student's *t*-test. (E) Release of a toxic factor by degenerating motor neurons evaluated in co-cultures of wild-type motor neurons from Hb9:GFP mice placed on top of control or alsin-depleted spinal motor neurons. (F) Diagram showing that there were no toxic effects of alsin-depleted spinal motor neurons on wild-type spinal motor neurons. Data show mean ± SD from $n = 4$ wells per condition. Each experiment was repeated twice yielding similar results.

factor released by spinal motor neurons and scavenged by astrocytes. To test the latter, we cultured alsin-depleted spinal motor neurons (potentially toxic) or control spinal motor neurons (non-toxic) on the bottom of the wells and 'indicator' motor neurons from Hb9:GFP mice (46) on the top coverslips (Fig. 4E). Survival of the indicator motor neurons was similar under both conditions (Fig. 4F) ruling out the release of a toxic factor. Taken together these data

indicate that astrocytes rescue alsin-depleted spinal motor neurons from cell death by releasing a diffusible factor.

To characterize the biochemical nature of the factor, we separated astrocytes and motor neurons in the co-cultures by semi-permeable dialysis membranes. Membranes with a molecular weight cut-off of 500 Da almost completely abrogated the astrocytic rescue effect (Supplementary Material, Fig. S2) reflecting the action of a higher molecular weight factor. We next prepared conditioned media from astrocyte monolayers. Neither lyophilized nor fresh astrocytic media were capable to rescue the survival of alsin-depleted spinal motor neurons (Supplementary Material, Fig. S2 and data not shown). We also tested the effect of blocking Rac1 activation. Expression of the dominant-negative Rac1 mutant T17N did not block the astrocytic rescue (data not shown). We finally checked whether the efficiency of RNAi in the neurons might be decreased by the co-cultured astrocytes. qRT–PCR analysis of alsin expression levels (Supplementary Material, Fig. S3) ruled out this possibility. The astrocytic factor thus most likely represents one or several molecules of molecular weight $>$ 500 Da that antagonize loss-of-alsin function at a downstream level.

Astrocytic rescue of axon growth defects in alsin-depleted spinal motor neurons

Axonal growth defects of different severity have been observed in alsin-deficient rat spinal motor neurons (38), mouse hippocampal neurons (39) and zebrafish spinal motor neurons (26). We therefore wondered whether axonal growth defects could also be rescued by the astrocyte-derived soluble factor. To test this, spinal motor neurons were cultured on coverslips separated from remote astrocyte monolayers, as before. After 2 DIV, neurons were fixed, imaged and the length of their axon, defined as the longest neurite, measured (Fig. 5A and B). In the absence of co-cultured astrocytes, alsin-depleted spinal motor neurons displayed a 37% reduction in mean axon length (123.8 $\pm$ 22.8 μm, mean $\pm$ SEM) when compared with control motor neurons (195.5 $\pm$ 15.5 μm, $P < 0.001$, Mann–Whitney rank sum test, Fig. 5C). There was no evidence of axonal swellings or blebs suggesting that alsin depletion retarded axon growth rather than induced axonal degeneration (Fig. 5A). In the presence of astrocytes, the mean axon length of alsin-depleted motor neurons (248.2 $\pm$ 23.7 μm) was restored to that of control spinal motor neurons (248.5 $\pm$ 25.6 μm) indicating complete astrocytic rescue. Cumulative plots (Fig. 5C) further showed that alsin-depleted spinal motor neurons with short axons $<$ 100 μm length were much less frequent in the presence of astrocytes (26%) than in their absence (68%). These observations indicate that the astrocyte-derived soluble factor rescues both survival and growth defects of alsin-depleted spinal motor neurons.

No astrocytic rescue of cortical neurons from alsin depletion triggered defects

We finally evaluated the response of cortical neurons to the astrocytic factor. Surprisingly, alsin-depleted cortical neurons could not be rescued from cell death by spinal astrocytes. Since astrocytes of distinct CNS regions differ in their functional properties, this failure might be specific for spinal astrocytes (33,47–50). We therefore also tested the potential rescue effects of cortical and hippocampal astrocytes. Astrocytes from cerebral cortex had a similar morphology as spinal astrocytes (Fig. 6A) and lacked alsin protein expression (Fig. 1D). They did not rescue alsin-depleted cortical neurons from decreased survival (Fig. 6C) or increased cell death (data not shown). Astrocytes from hippocampus, a region displaying gliosis in alsin knockout mice (22), also failed to induce rescue (Fig. 6D). In contrast, both types of astrocytes completely rescued alsin-depleted spinal motor neurons (data not shown).

Cell body survival and axon growth/maintenance are regulated by distinct extracellular triggers and intracellular pathways which vary between neuronal cell types (51). We therefore also determined the axon growth of cortical neurons following alsin depletion. In comparison to controls, the mean axon length of alsin-depleted cortical neurons at 2 DIV (Fig. 6E) was reduced by 42% ($P < 0.0001$, Mann–Whitney rank sum test), a value close to that observed for spinal motor neurons. The axon growth defect of cortical neurons was, however, not rescued by co-cultured astrocytes (Fig. 6E). Taken together, the data indicate that cortical neurons have a similar intrinsic vulnerability to loss-of-alsin function as spinal motor neurons but are insensitive to astrocytic rescue.

DISCUSSION

Glial cell hypertrophy and proliferation are hallmarks of degenerative motor neuron diseases such as ALS. They are typically found in affected regions, i.e. in the vicinity of cortical and spinal motor neurons and around degenerating corticospinal axons and their entry points into the grey matter (27–29). Astrocytes represent the most abundant glial cell population in spinal cord and brain (52) and contribute to many homeostatic functions potentially involved in motor neuron maintenance (reviewed in 41,42). These include clearance of extracellular glutamate, maintenance of extracellular ion concentration and fluid balance, production of glucose and other energy metabolites, scavenging of free radicals and production of neurotrophic factors. Astrocytes also play important roles in intercellular communication, e.g. by rapidly propagating calcium waves through interconnected gap junctions (53) and by bridging neurons, glia and vascular cells (42). On the other hand, astrocytes can release various pro-inflammatory and pro-apoptotic factors such as IL6, TNF-α, FasL and reactive oxygen and nitrogen species such as nitric oxide and peroxynitrite (reviewed in 35). Given these multiple functions, astrocytes can, in principle, be beneficial or detrimental for motor neuron maintenance.

We report that astrocytes completely rescue the survival and axon growth defects of co-cultured spinal motor neurons in a cellular Als2/alsin loss-of-function model. This rescue represents a genuine astrocytic function, because it is exerted by astrocytes from various anatomic origins which do not express alsin. Our data further indicate that astrocytic rescue of alsin-depleted spinal motor neurons is mediated by release of a soluble neuroprotective factor rather than by scavenging

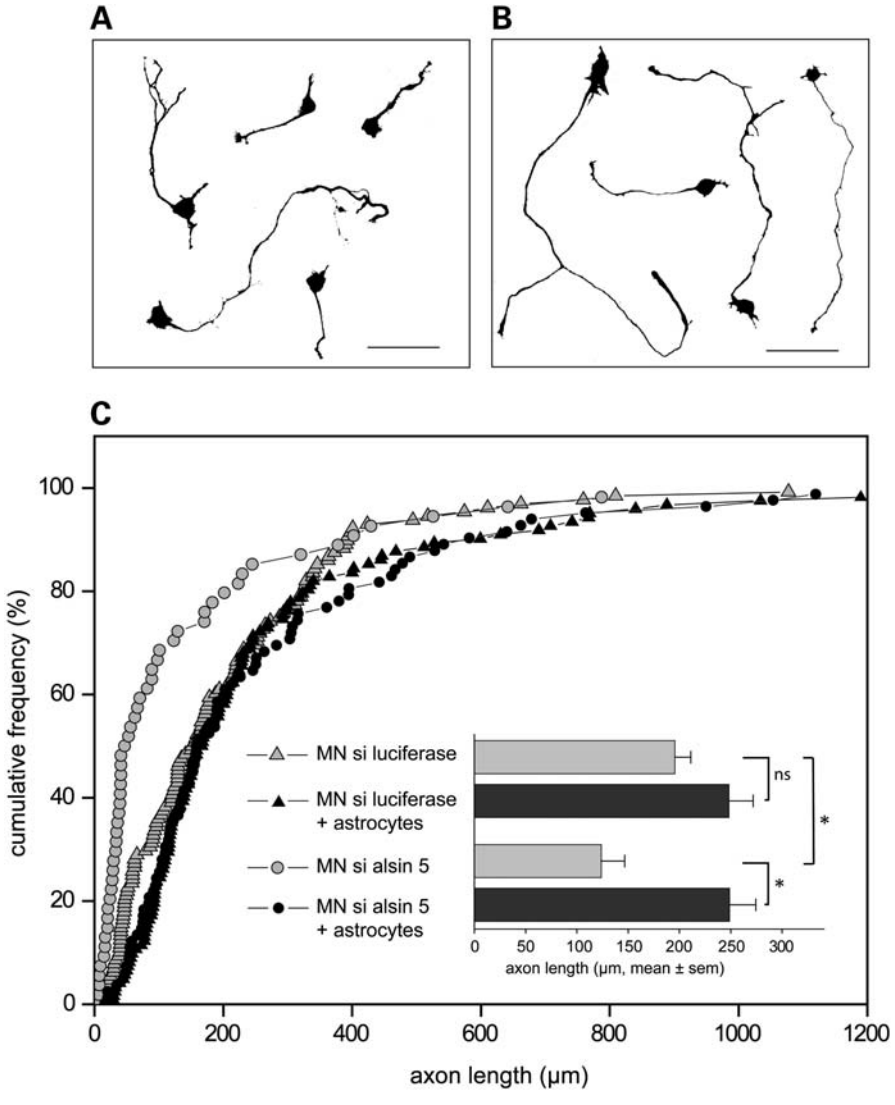

Figure 5. Astrocytes rescue defective axon growth of alsin-depleted spinal motor neurons. Spinal motor neurons (MN) were electroporated with si luciferase/GFP plasmid or si alsin 5/GFP plasmid and grown on coverslips placed on top of empty wells or on wells containing astrocyte monolayers. (**A** and **B**) Representative examples of GFP-fluorescent alsin-depleted spinal motor neurons in the absence (A) or presence (B) of astrocytes. Scale bar 50 µm. (**C**) Cumulative plot showing defective axon length of alsin-depleted spinal motor neurons and its rescue by astrocytes. Bar diagrams (inset) showing that axon growth of si luciferase spinal motor neurons is not significantly increased by the presence of astrocytes (ns, $P = 0.1$). In contrast, mean axon length of alsin-depleted spinal motor neurons is increased by 93% ($^*P < 0.001$, Mann–Whitney rank sum test). Number of spinal motor neurons analyzed: MN si alsin, $n = 64$; MN si alsin 5 + astrocytes: $n = 92$; MN si luciferase: $n = 128$, MN si luciferase + astrocytes, $n = 122$. Shown are data from one out of two independent experiments which yielded similar results.

of a toxic factor derived from motor neurons or by cellular contact. What might be the nature of the astrocytic factor? We estimate that the astrocytic factor has a molecular weight of >500 Da. Potential candidates are neurotrophic factors (54,55) and cytokines (56). We also show that the factor is biologically unstable making its biochemical identification challenging. Which intracellular signalling pathways are involved in the astrocytic protection? Alsin survival signalling in motor neurons strictly depends on Rac1 activation (38) and might involve phosphatidylinositol 3-kinase and Akt as downstream effectors (9). Here we show that the astrocytic rescue of alsin-depleted spinal motor neurons does not depend on Rac1 activation. Future studies will determine at which downstream level the astrocyte-triggered protective pathway interferes with the alsin depletion triggered cell death pathway.

To our knowledge, the present study provides the first example of non-cell autonomous astrocytic effects in a non-SOD1-linked ALS model. There are however mechanistic differences. First, the 184 kDa alsin protein is predominantly expressed in neurons, whereas mutant SOD1 is ubiquitously expressed including in astrocytes (1,2). Secondly, rather than being protective, mutant SOD1 expressing astrocytes are detrimental to co-cultured motor neurons. This might involve release of toxic factors (31,32) inducing Caspase-3 and Bax-dependent cell death (31) or defective release of factors modulating glutamate receptor subunit composition (33) of

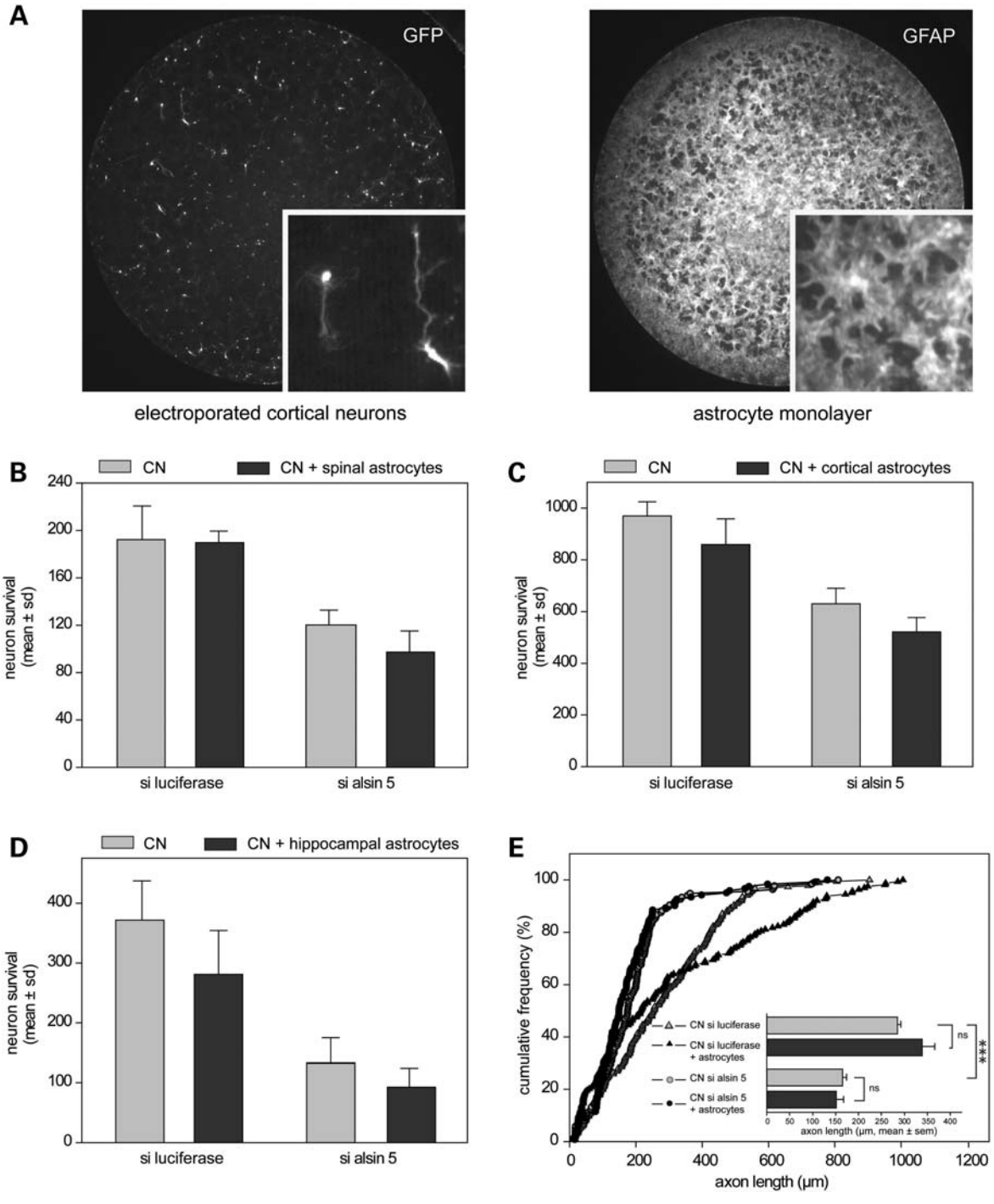

Figure 6. Astrocytes do not rescue alsin-depleted cortical neurons. (**A**) Images of GFP-fluorescent cortical neurons (CN) cultured on pre-established cortical astrocytes visualized by GFAP immunostaining. (**B**–**D**) Diagrams showing survival analyses. Spinal, cortical and hippocampal astrocytes were unable to protect cortical neurons against cell death induced by alsin depletion. Experimental conditions were identical to those for spinal motor neuron/astrocyte co-cultures (Fig. 3C) in order to allow for comparison. (**E**) Cumulative plot and bar diagrams (inset) showing axon length analyses. Cortical neurons were cultured on top coverslips in six-well dishes. In the absence of co-cultured astrocytes, alsin-depleted cortical neurons growth show shorter axons than control neurons ($^{***}P < 0.001$). In the presence of co-cultured astrocytes, there is no rescue of defective axon growth (ns, $P > 0.5$). Values represent mean ± SEM from one representative out of two independent experiments. Statistical analyses were done with Mann–Whitney rank sum test. Number of cortical neurons analyzed per condition: CN si luciferase: $n = 186$; CN si luciferase + astrocytes, $n = 164$, CN si alsin, $n = 136$; CN si alsin 5 + astrocytes: $n = 122$.

motor neurons. Thirdly, the factors released by mutant SOD1 expressing astrocytes are biologically stable (31,33), in contrast to the astrocytic factor rescuing alsin-depleted spinal motor neurons. These functional differences warrant the study of astrocytic/motor neuron interactions in additional models of motor neuron disease.

Genetic forms of motor neuron diseases often display considerable intrafamilial heterogeneity suggesting the existence of modifier genes or disease-modulating factors. In a Brazilian population, the same dominantly inherited mutation (P56S) in vesicle-associated membrane protein-associated protein B (VAPB) was associated with three different phenotypes: typical ALS with pyramidal tract and upper motor neuron signs, atypical ALS with essential tremor and late-onset spinal muscular atrophy (57). Recessive mutations in ALS2/Alsin have been associated with atypical juvenile forms of ALS and JPLS and infantile forms of IAHSP (13–20). In humans and mice, loss of ALS2/Alsin function seems to more consistently affect cortical rather than spinal motor neurons. In a large consanguineous family, all twelve members carrying the same Alsin mutation exhibited upper motor neuron symptoms but few had clear evidence of lower motor neuron involvement (58). In alsin knockout mice, the degeneration of cortical motor neurons, attested by large axonal swellings (24,25), seemed more severe than the degeneration of spinal motor neurons, attested principally by axonal transport defects (26) and motor unit remodelling (22). Our data show that cortical neurons have a similar intrinsic vulnerability to loss-of-alsin as spinal motor neurons but are insensitive to astrocytic rescue. We therefore propose that astrocytes act as cellular disease modifiers accounting for the relative preservation of lower motor neurons in human Alsin/ALS2-linked neurodegenerative diseases. Elucidating the molecular mechanisms of astrocytic neuroprotection may also help to conceive new therapeutic strategies for these severe diseases.

MATERIALS AND METHODS

RNAi duplexes and plasmid vectors

siRNAs targeting alsin were designed manually [si alsin 5 sense: GAUACUUAGGCCUCUUCUCd(TT); si alsin 6 sense: AGCAGCAGGAUUCCAGUUCUd(TT)] and duplexes purchased from Qiagen (HPP grade). siRNA targeting luciferase (siGL2, Qiagen) was used as control. The pCAGGS GFP expression vector has been described (38).

Neuronal and glial cell cultures

NSC34 cells (40) were cultured in plastic dishes coated with polyornithin using Dulbecco's minimum essential medium (DMEM; Invitrogen, La Jolla, CA, USA) supplemented with 10% fetal calf serum (Invitrogen).

Spinal motor neurons were prepared from E12 Swiss mice, essentially as described (59), and cultured in supplemented Neurobasal medium without Riboflavin (Invitrogen) containing 2% B27, 2% horse serum, 500 μM glutamine, 25 μM beta-mercaptoethanol, 1 ng/ml BDNF, 1 ng/ml GDNF, 10 ng/ml CNTF and 10 IU/ml penicillin–streptomycin (Invitrogen).

Cortical neurons were prepared from E15 Swiss mice. After decapitation, cortices were rapidly removed and placed in 35 mm Petri dishes containing sterile HBSS (Invitrogen). The meninges surrounding the tissues were removed, and the neurons were dissociated by trypsin digestion. Neurons were plated at a density of 70 000 cells/cm^2 in six-well plate or coverslips coated with polyornithin in Neurobasal medium (Invitrogen) supplemented with 2% B27, 2% horse serum, 2 mM glutamine, 1 ng/ml BDNF, 1 ng/ml GDNF, 10 ng/ml CNTF and 10 IU/ml penicillin–streptomycin (Invitrogen).

Hippocampal neurons were prepared from E17 Swiss mice as described (60). Briefly, embryos were decapitated, the CA1–CA3 regions of hippocampi rapidly removed and placed in 35 mm Petri dishes containing sterile HBSS buffer. The meninges surrounding the tissues were removed, the cells dissociated by trypsin and plated at a density of 70 000 cells/cm^2 in six-well plate or coverslips coated with polyornithin. Neurons were cultured in Neurobasal medium supplemented with 2% B27, 0.8% glucose, 1 mM sodium pyruvate, 2 mM glutamine, 1 ng/ml BDNF, 1 ng/ml GDNF, 10 ng/ml CNTF and 10 IU/ml penicillin–streptomycin.

Type I astrocytes were generated as described (61). Briefly, cortices, hippocampi or spinal cords were dissected from P2–P4 mice, freed from meninges, incubated with 0.25% trypsin and 0.5 mM EDTA (Invitrogen) and triturated. Cells were cultured in T-75 flasks containing DMEM supplemented with 10% (vol/vol) fetal calf serum. At cell confluence, the flasks were shaken at 300 tours/min for 16 h to remove neurons, oligodendrocytes and microglia. After two to three passages, the cultures contained > 95% GFAP-positive cells.

Transfection and electroporation

NSC34 cells were transfected with Lipofectamine 2000 according to the manufacturer's instructions (Invitrogen). Neurons and astrocytes were electroporated as described previously (38). Briefly, cells were pelleted and re-suspended in electroporation buffer (125 mM NaCl, 5 mM KCl, 1.5 mM $MgCl_2$, 10 mM glucose, 20 mM HEPES, pH7.4). For RNAi experiments, cells were incubated with siRNA (4 pmol/μl) together with pCAGGS GFP DNA plasmid (5 μg). After 15 min incubation at room temperature, the cell suspensions were transferred to a 4 mm gap cuvette and electroporated using a BTX-ECM830 electroporator (Genetronics, San Diego, CA, USA). Electroporation conditions were three square pulses of 5 ms at 200 V each with intervals of 1 s. Cells were then re-suspended in culture medium and seeded on glass coverslips, 96-well plastic dishes (Greiner Bio-One, Longwood, FL, ref. 655090) or 6-well plastic dishes (Nunc) coated with polyornithin/laminin.

Co-cultures of neurons and astrocytes

Astrocytes were seeded in half of the wells of a 96-well plate (Greiner) and cultured to confluence. Wells were then washed twice with PBS to eliminate all traces of astrocyte growth medium and electroporated neurons seeded in wells containing the astrocyte monolayer or in neighbouring empty wells. Remote neuron–astrocyte co-cultures were prepared by modifying a previously described technique (61). In six-well dishes (Nunc), three wells were used to culture astrocytes to confluence and three others were left empty. Electroporated neurons were seeded on polyornithin/laminin-coated glass coverslips (12 mm) that had been previously fitted with paraffin wax stilts. Once the neurons had adhered, the fitted coverslips

were placed into the dishes containing (or not) the astrocyte monolayers. All co-cultures were performed in Neurobasal medium (Invitrogen) containing 2% B27 supplement, 2% horse serum, 500 μM glutamine, 25 μM beta-mercaptoethanol, 1 ng/ml BDNF, 1 ng/ml GDNF, 10 ng/ml CNTF and 10 IU/ml penicillin–streptomycin (Invitrogen).

Immunoblot and qRT–PCR analyses

For immunoblot analysis, total proteins from primary cell cultures were extracted with lysis buffer containing 50 mM tris[hydroxymethyl]aminomethane, pH 7.5, 150 mM NaCl, 2 mM EDTA, 2 mM EGTA, 1% Triton X-100 and complete protease inhibitor cocktail (Roche), denatured in sample buffer, subjected to sodium dodecyl sulphate polyacrylamide gel electrophoresis, and transferred onto a polyvinyl difluoride membrane (Millipore, Bedford, MA, USA). Blots were hybridized with antibodies against alsin (1:1000, a kind gift of C. Miller) or anti-alpha tubulin (1:20 000, Sigma) and with peroxidase-conjugated anti-rabbit or anti-mouse IgG goat secondary antibody (Jackson Immunoresearch Laboratories) and revealed using enzyme chemiluminescence plus kit (Amersham Pharmacia, Buckinghamshire, UK).

qRT–PCR was performed using SYBR green and analyzed with the Applied Biosystems 5700 Sequence Detector (Foster City, CA, USA) as described (62). The sequences of primers used for RT–PCR were as follows (5′ to 3′): mouse alsin exon 4 forward: ATGAGCCTGGAGAAAAGC; mouse alsin exon 5 reverse: TTGTGGTTGGTGGACTGT; mouse alsin exon 17 forward: CTCATTTCTTCAACACCCCA; mouse alsin exon 18 reverse: GCTTGGCTGATAGCCCGA; mouse ARPO forward: TCCAGAGGCACCATTGAAATT; mouse ARPO reverse: TCGCTGGCTCCCACCTT.

Immunocytochemistry

Primary cultures were fixed with 3.7% formaldehyde and processed for immunocytochemistry as described (59). Primary antibodies were anti-βIII tubulin (mouse, TuJ1, Eurogentec, 1:1000), anti-GFAP (rabbit, G4546, Sigma, 1:500). Secondary antibodies were anti-rabbit or anti-mouse-IgG antibodies conjugated to Alexa-488 or Cy3 (Jackson ImmunoResearch). Imaging was done with a Zeiss 510 confocal microscope using 10×, 20× and 40× objectives.

Assays for neuronal survival, death and axonal length

Survival of siRNA/GFP expressing neurons in 96-well plates was monitored using a Flash-cytometer (Trophos, Marseille) and TINA software. This system allows to determine the number of fluorescent objects per well and to quantify signal intensity of each detected object. Proportion of GFP fluorescent cells was ∼10% for spinal motor neurons and up to 30% for cortical neurons. Survival of motor neurons cultured on coverslips was analyzed after fixation with 3.7% (vol/vol) formaldehyde in PBS. The number of fluorescent cells was determined using an inverted microscope (Nikon Diaphot 300, 10× objective, Nikon, Melville, NY, USA or Zeiss Axio Observer D1, 10× objective, Zeiss, Jena, Germany).

Cell death of cultured neurons was analyzed using EthD-1 labelling. In brief, neuronal cultures were incubated with EthD-1 (Molecular Probes, ref. L3224) at a concentration of 0.25 μM in Neurobasal for 15 min at 37°C in the CO_2 incubator. After washing with PBS, GFP-positive live cells and EthD-1/GFP double-positive dead cells were counted and imaged using a Zeiss Axio Observer D1 microscope (20× objective) equipped with a Zeiss digital camera.

Axon length of cultured neurons was determined by acquiring images of randomly selected cells. At least 100 fluorescent neurons per condition were analyzed using the NeuronJ plugin of ImageJ software (National Center for Biotechnology Information, Bethesda, MD, USA).

Statistical analyses

Cultures in four-well plates were performed in duplicate or triplicate. Cultures in 96-well plates were done in eight parallel wells per condition. Data were analyzed with SigmaStat 3.1 software (Systat, San Jose, CA, USA). Data showing a Gaussian distribution were analyzed with Student's *t*-test (two-tailed, unpaired) or with two-way ANOVA; otherwise the Mann–Whitney rank sum test was used.

SUPPLEMENTARY MATERIAL

Supplementary Material is available at *HMG* online.

ACKNOWLEDGEMENTS

We thank Dr Chris Miller for providing anti-alsin antibodies, C. Pellegrino for advice with astrocyte cultures, Drs Igor Medina, Christophe Béclin, Odile Boespflug-Tanguy and members of the Haase Lab for helpful discussions.

Conflict of Interest statement. None declared.

FUNDING

The study was funded by grants from INSERM (Avenir program, G.H.), Agence Nationale pour la Recherche (Motoaxone, G.H.) and Association Française contre les Myopathies (MN11452/12535, G.H.). The author's laboratories were also supported by grants from Fédération pour la Recherche sur le Cerveau (G.H.), Région Provence-Alpes-Côte d'Azur (G.H.), European Union (G.H.) and Association pour la Recherche sur la Sclérose Laterale Amyotrophique (D.B.). A.J. was recipient of a PhD fellowship from INSERM/Région Provence-Alpes-Côte d'Azur and Fondation pour la Recherche Médicale (FRM). S.B. is recipient of an ANR fellowship.

REFERENCES

1. Pasinelli, P. and Brown, R.H. (2006) Molecular biology of amyotrophic lateral sclerosis: insights from genetics. *Nat. Rev. Neurosci.*, **7**, 710–723.
2. Boillee, S., Vande Velde, C. and Cleveland, D.W. (2006) ALS: a disease of motor neurons and their nonneuronal neighbors. *Neuron*, **52**, 39–59.
3. Hadano, S., Kunita, R., Otomo, A., Suzuki-Utsunomiya, K. and Ikeda, J.E. (2007) Molecular and cellular function of ALS2/alsin: implication of

membrane dynamics in neuronal development and degeneration. *Neurochem. Int.*, **51**, 74–84.
4. Chandran, J., Ding, J. and Cai, H. (2007) Alsin and the molecular pathways of amyotrophic lateral sclerosis. *Mol. Neurobiol.*, **36**, 224–231.
5. Lesca, G., Eymard-Pierre, E., Santorelli, F.M., Cusmai, R., Di Capua, M., Valente, E.M., Attia-Sobol, J., Plauchu, H., Leuzzi, V., Ponzone, A. *et al.* (2003) Infantile ascending hereditary spastic paralysis (IAHSP): clinical features in 11 families. *Neurology*, **60**, 674–682.
6. Yamanaka, K., Vande Velde, C., Eymard-Pierre, E., Bertini, E., Boespflug-Tanguy, O. and Cleveland, D.W. (2003) Unstable mutants in the peripheral endosomal membrane component ALS2 cause early-onset motor neuron disease. *Proc. Natl Acad. Sci. USA*, **100**, 16041–16046.
7. Kunita, R., Otomo, A., Mizumura, H., Suzuki, K., Showguchi-Miyata, J., Yanagisawa, Y., Hadano, S. and Ikeda, J.E. (2004) Homo-oligomerization of ALS2 through its unique carboxyl-terminal regions is essential for the ALS2-associated Rab5 guanine nucleotide exchange activity and its regulatory function on endosome trafficking. *J. Biol. Chem.*, **279**, 38626–38635.
8. Otomo, A., Hadano, S., Okada, T., Mizumura, H., Kunita, R., Nishijima, H., Showguchi-Miyata, J., Yanagisawa, Y., Kohiki, E., Suga, E. *et al.* (2003) ALS2, a novel guanine nucleotide exchange factor for the small GTPase Rab5, is implicated in endosomal dynamics. *Hum. Mol. Genet.*, **12**, 1671–1687.
9. Kanekura, K., Hashimoto, Y., Kita, Y., Sasabe, J., Aiso, S., Nishimoto, I. and Matsuoka, M. (2005) A Rac1/phosphatidylinositol 3-kinase/Akt3 anti-apoptotic pathway, triggered by AlsinLF, the product of the *ALS2* gene, antagonizes Cu/Zn-superoxide dismutase (SOD1) mutant-induced motoneuronal cell death. *J. Biol. Chem.*, **280**, 4532–4543.
10. Topp, J.D., Gray, N.W., Gerard, R.D. and Horazdovsky, B.F. (2004) Alsin is a Rab5 and Rac1 guanine nucleotide exchange factor. *J. Biol. Chem.*, **279**, 24612–24623.
11. Tudor, E.L., Perkinton, M.S., Schmidt, A., Ackerley, S., Brownlees, J., Jacobsen, N.J., Byers, H.L., Ward, M., Hall, A., Leigh, P.N. *et al.* (2005) ALS2/alsin regulates Rac-PAK signaling and neurite outgrowth. *J. Biol. Chem.*, **280**, 34735–34740.
12. Kunita, R., Otomo, A., Mizumura, H., Suzuki-Utsunomiya, K., Hadano, S. and Ikeda, J.E. (2007) The Rab5 activator ALS2/alsin acts as a novel Rac1 effector through Rac1-activated endocytosis. *J. Biol. Chem.*, **282**, 16599–16611.
13. Eymard-Pierre, E., Lesca, G., Dollet, S., Santorelli, F.M., di Capua, M., Bertini, E. and Boespflug-Tanguy, O. (2002) Infantile-onset ascending hereditary spastic paralysis is associated with mutations in the alsin gene. *Am. J. Hum. Genet.*, **71**, 518–527.
14. Eymard-Pierre, E., Yamanaka, K., Haeussler, M., Kress, W., Gauthier-Barichard, F., Combes, P., Cleveland, D.W. and Boespflug-Tanguy, O. (2006) Novel missense mutation in *ALS2* gene results in infantile ascending hereditary spastic paralysis. *Ann. Neurol.*, **59**, 976–980.
15. Verschuuren-Bemelmans, C.C., Winter, P., Sival, D.A., Elting, J.W., Brouwer, O.F. and Muller, U. (2008) Novel homozygous ALS2 nonsense mutation (p.Gln715X) in sibs with infantile-onset ascending spastic paralysis: the first cases from northwestern Europe. *Eur. J. Hum. Genet.*, **16**, 1407–1411.
16. Gros-Louis, F., Meijer, I.A., Hand, C.K., Dube, M.P., MacGregor, D.L., Seni, M.H., Devon, R.S., Hayden, M.R., Andermann, F., Andermann, E. *et al.* (2003) An *ALS2* gene mutation causes hereditary spastic paraplegia in a Pakistani kindred. *Ann. Neurol.*, **53**, 144–145.
17. Devon, R.S., Helm, J.R., Rouleau, G.A., Leitner, Y., Lerman-Sagie, T., Lev, D. and Hayden, M.R. (2003) The first nonsense mutation in alsin results in a homogeneous phenotype of infantile-onset ascending spastic paralysis with bulbar involvement in two siblings. *Clin. Genet.*, **64**, 210–215.
18. Hadano, S., Hand, C.K., Osuga, H., Yanagisawa, Y., Otomo, A., Devon, R.S., Miyamoto, N., Showguchi-Miyata, J., Okada, Y., Singaraja, R. *et al.* (2001) A gene encoding a putative GTPase regulator is mutated in familial amyotrophic lateral sclerosis 2. *Nat. Genet.*, **29**, 166–173.
19. Yang, Y., Hentati, A., Deng, H.X., Dabbagh, O., Sasaki, T., Hirano, M., Hung, W.Y., Ouahchi, K., Yan, J., Azim, A.C. *et al.* (2001) The gene encoding alsin, a protein with three guanine-nucleotide exchange factor domains, is mutated in a form of recessive amyotrophic lateral sclerosis. *Nat. Genet.*, **29**, 160–165.
20. Kress, J.A., Kuhnlein, P., Winter, P., Ludolph, A.C., Kassubek, J., Muller, U. and Sperfeld, A.D. (2005) Novel mutation in the *ALS2* gene in juvenile amyotrophic lateral sclerosis. *Ann. Neurol.*, **58**, 800–803.
21. Cai, H., Lin, X., Xie, C., Laird, F.M., Lai, C., Wen, H., Chiang, H.C., Shim, H., Farah, M.H., Hoke, A. *et al.* (2005) Loss of ALS2 function is insufficient to trigger motor neuron degeneration in knock-out mice but predisposes neurons to oxidative stress. *J. Neurosci.*, **25**, 7567–7574.
22. Hadano, S., Benn, S.C., Kakuta, S., Otomo, A., Sudo, K., Kunita, R., Suzuki-Utsunomiya, K., Mizumura, H., Shefner, J.M., Cox, G.A. *et al.* (2006) Mice deficient in the Rab5 guanine nucleotide exchange factor ALS2/alsin exhibit age-dependent neurological deficits and altered endosome trafficking. *Hum. Mol. Genet.*, **15**, 233–250.
23. Devon, R.S., Orban, P.C., Gerrow, K., Barbieri, M.A., Schwab, C., Cao, L.P., Helm, J.R., Bissada, N., Cruz-Aguado, R., Davidson, T.L. *et al.* (2006) Als2-deficient mice exhibit disturbances in endosome trafficking associated with motor behavioral abnormalities. *Proc. Natl Acad. Sci. USA*, **103**, 9595–9600.
24. Deng, H.X., Zhai, H., Fu, R., Shi, Y., Gorrie, G.H., Yang, Y., Liu, E., Dal Canto, M.C., Mugnaini, E. and Siddique, T. (2007) Distal axonopathy in an alsin-deficient mouse model. *Hum. Mol. Genet.*, **16**, 2911–2920.
25. Yamanaka, K., Miller, T.M., McAlonis-Downes, M., Chun, S.J. and Cleveland, D.W. (2006) Progressive spinal axonal degeneration and slowness in ALS2-deficient mice. *Ann. Neurol.*, **60**, 95–104.
26. Gros-Louis, F., Kriz, J., Kabashi, E., McDearmid, J., Millecamps, S., Urushitani, M., Lin, L., Dion, P., Zhu, Q., Drapeau, P. *et al.* (2008) Als2 mRNA splicing variants detected in KO mice rescue severe motor dysfunction phenotype in Als2 knockdown zebrafish. *Hum. Mol. Genet.*, **17**, 2691–2702.
27. Hirano, A. (1996) Neuropathology of ALS: an overview. *Neurology*, **47**, S63–S66.
28. Kushner, P.D., Stephenson, D.T. and Wright, S. (1991) Reactive astrogliosis is widespread in the subcortical white matter of amyotrophic lateral sclerosis brain. *J. Neuropathol. Exp. Neurol.*, **50**, 263–277.
29. Schiffer, D., Cordera, S., Cavalla, P. and Migheli, A. (1996) Reactive astrogliosis of the spinal cord in amyotrophic lateral sclerosis. *J. Neurol. Sci.*, **139** (suppl.), 27–33.
30. Yamanaka, K., Chun, S.J., Boillee, S., Fujimori-Tonou, N., Yamashita, H., Gutmann, D.H., Takahashi, R., Misawa, H. and Cleveland, D.W. (2008) Astrocytes as determinants of disease progression in inherited amyotrophic lateral sclerosis. *Nat. Neurosci.*, **11**, 251–253.
31. Nagai, M., Re, D.B., Nagata, T., Chalazonitis, A., Jessell, T.M., Wichterle, H. and Przedborski, S. (2007) Astrocytes expressing ALS-linked mutated SOD1 release factors selectively toxic to motor neurons. *Nat. Neurosci.*, **10**, 615–622.
32. Di Giorgio, F.P., Carrasco, M.A., Siao, M.C., Maniatis, T. and Eggan, K. (2007) Non-cell autonomous effect of glia on motor neurons in an embryonic stem cell-based ALS model. *Nat. Neurosci.*, **10**, 608–614.
33. Van Damme, P., Bogaert, E., Dewil, M., Hersmus, N., Kiraly, D., Scheveneels, W., Bockx, I., Braeken, D., Verpoorten, N., Verhoeven, K. *et al.* (2007) Astrocytes regulate GluR2 expression in motor neurons and their vulnerability to excitotoxicity. *Proc. Natl Acad. Sci. USA*, **104**, 14825–14830.
34. Haase, G., Pettmann, B., Raoul, C. and Henderson, C.E. (2008) Signaling by death receptors in the nervous system. *Curr. Opin. Neurobiol.*, **18**, 284–291.
35. Barbeito, L.H., Pehar, M., Cassina, P., Vargas, M.R., Peluffo, H., Viera, L., Estevez, A.G. and Beckman, J.S. (2004) A role for astrocytes in motor neuron loss in amyotrophic lateral sclerosis. *Brain Res. Brain Res. Rev.*, **47**, 263–274.
36. Devon, R.S., Schwab, C., Topp, J.D., Orban, P.C., Yang, Y.Z., Pape, T.D., Helm, J.R., Davidson, T.L., Rogers, D.A., Gros-Louis, F. *et al.* (2005) Cross-species characterization of the *ALS2* gene and analysis of its pattern of expression in development and adulthood. *Neurobiol. Dis.*, **18**, 243–257.
37. Lai, C., Xie, C., McCormack, S.G., Chiang, H.C., Michalak, M.K., Lin, X., Chandran, J., Shim, H., Shimoji, M., Cookson, M.R. *et al.* (2006) Amyotrophic lateral sclerosis 2-deficiency leads to neuronal degeneration in amyotrophic lateral sclerosis through altered AMPA receptor trafficking. *J. Neurosci.*, **26**, 11798–11806.
38. Jacquier, A., Buhler, E., Schafer, M.K., Bohl, D., Blanchard, S., Beclin, C. and Haase, G. (2006) Alsin/Rac1 signaling controls survival and growth of spinal motoneurons. *Ann. Neurol.*, **60**, 105–117.

39. Otomo, A., Kunita, R., Suzuki-Utsunomiya, K., Mizumura, H., Onoe, K., Osuga, H., Hadano, S. and Ikeda, J.E. (2008) ALS2/alsin deficiency in neurons leads to mild defects in macropinocytosis and axonal growth. *Biochem. Biophys. Res. Commun.*, **370**, 87–92.
40. Cashman, N.R., Durham, H.D., Blusztajn, J.K., Oda, K., Tabira, T., Shaw, I.T., Dahrouge, S. and Antel, J.P. (1992) Neuroblastoma x spinal cord (NSC) hybrid cell lines resemble developing motor neurons. *Dev. Dyn.*, **194**, 209–221.
41. Maragakis, N.J. and Rothstein, J.D. (2006) Mechanisms of disease: astrocytes in neurodegenerative disease. *Nat. Clin. Pract. Neurol.*, **2**, 679–689.
42. Volterra, A. and Meldolesi, J. (2005) Astrocytes, from brain glue to communication elements: the revolution continues. *Nat. Rev. Neurosci.*, **6**, 626–640.
43. Kimura, K., Matsumoto, N., Kitada, M., Mizoguchi, A. and Ide, C. (2004) Neurite outgrowth from hippocampal neurons is promoted by choroid plexus ependymal cells *in vitro*. *J. Neurocytol.*, **33**, 465–476.
44. Dotti, C.G., Sullivan, C.A. and Banker, G.A. (1988) The establishment of polarity by hippocampal neurons in culture. *J. Neurosci.*, **8**, 1454–1468.
45. Ozdinler, P.H. and Macklis, J.D. (2006) IGF-I specifically enhances axon outgrowth of corticospinal motor neurons. *Nat. Neurosci.*, **9**, 1371–1381.
46. Wichterle, H., Lieberam, I., Porter, J.A. and Jessell, T.M. (2002) Directed differentiation of embryonic stem cells into motor neurons. *Cell*, **110**, 385–397.
47. Wagner, B., Natarajan, A., Grunaug, S., Kroismayr, R., Wagner, E.F. and Sibilia, M. (2006) Neuronal survival depends on EGFR signaling in cortical but not midbrain astrocytes. *EMBO J.*, **25**, 752–762.
48. Sousa Vde, O., Romao, L., Neto, V.M. and Gomes, F.C. (2004) Glial fibrillary acidic protein gene promoter is differently modulated by transforming growth factor-beta 1 in astrocytes from distinct brain regions. *Eur. J. Neurosci.*, **19**, 1721–1730.
49. Autillo-Touati, A., Chamak, B., Araud, D., Vuillet, J., Seite, R. and Prochiantz, A. (1988) Region-specific neuro-astroglial interactions: ultrastructural study of the *in vitro* expression of neuronal polarity. *J. Neurosci. Res.*, **19**, 326–342.
50. Barbin, G., Katz, D.M., Chamak, B., Glowinski, J. and Prochiantz, A. (1988) Brain astrocytes express region-specific surface glycoproteins in culture. *Glia*, **1**, 96–103.
51. Coleman, M. (2005) Axon degeneration mechanisms: commonality amid diversity. *Nat. Rev. Neurosci.*, **6**, 889–898.
52. Wilkin, G.P., Marriott, D.R. and Cholewinski, A.J. (1990) Astrocyte heterogeneity. *Trends Neurosci.*, **13**, 43–46.
53. Giaume, C. and Venance, L. (1998) Intercellular calcium signaling and gap junctional communication in astrocytes. *Glia*, **24**, 50–64.
54. Eagleson, K.L., Raju, T.R. and Bennett, M.R. (1985) Motoneurone survival is induced by immature astrocytes from developing avian spinal cord. *Brain Res.*, **349**, 95–104.
55. Yin, Q.W., Johnson, J., Prevette, D. and Oppenheim, R.W. (1994) Cell death of spinal motoneurons in the chick embryo following deafferentation: rescue effects of tissue extracts, soluble proteins, and neurotrophic agents. *J. Neurosci.*, **14**, 7629–7640.
56. Dhandapani, K.M., Wade, F.M., Mahesh, V.B. and Brann, D.W. (2005) Astrocyte-derived transforming growth factor-{beta} mediates the neuroprotective effects of 17{beta}-estradiol: involvement of nonclassical genomic signaling pathways. *Endocrinology*, **146**, 2749–2759.
57. Nishimura, A.L., Mitne-Neto, M., Silva, H.C., Richieri-Costa, A., Middleton, S., Cascio, D., Kok, F., Oliveira, J.R., Gillingwater, T., Webb, J. *et al.* (2004) A mutation in the vesicle-trafficking protein VAPB causes late-onset spinal muscular atrophy and amyotrophic lateral sclerosis. *Am. J. Hum. Genet.*, **75**, 822–831.
58. Ben Hamida, M., Hentati, F. and Ben Hamida, C. (1990) Hereditary motor system diseases (chronic juvenile amyotrophic lateral sclerosis). Conditions combining a bilateral pyramidal syndrome with limb and bulbar amyotrophy. *Brain*, **113**, 347–363.
59. Raoul, C., Estevez, A.G., Nishimune, H., Cleveland, D.W., deLapeyriere, O., Henderson, C.E., Haase, G. and Pettmann, B. (2002) Motoneuron death triggered by a specific pathway downstream of Fas. Potentiation by ALS-linked SOD1 mutations. *Neuron*, **35**, 1067–1083.
60. Krapivinsky, G., Krapivinsky, L., Manasian, Y., Ivanov, A., Tyzio, R., Pellegrino, C., Ben-Ari, Y., Clapham, D.E. and Medina, I. (2003) The NMDA receptor is coupled to the ERK pathway by a direct interaction between NR2B and RasGRF1. *Neuron*, **40**, 775–784.
61. Goslin, K. and Banker, G. (1991) Rat hippocanpal neurons in low-density culture. In Banker, G. and Goslin, K. (eds), *Culturing Nerve Cells*. MIT Press, Cambridge, pp. 207–226.
62. Bohl, D., Liu, S., Blanchard, S., Hocquemiller, M., Haase, G. and Heard, J.M. (2008) Directed evolution of motor neurons from genetically engineered neural precursors. *Stem Cells*, **26**, 2564–2575.